Theoretical study of electron confinement in Cu corrals on a Cu(111) surface

Sergio Díaz-Tendero,[1,2] Fredrik E. Olsson,[3] Andrey G. Borisov,[1,2] and Jean-Pierre Gauyacq[1,2,*]
[1]*CNRS, Laboratoire des Collisions Atomiques et Moléculaires, UMR 8625, Bâtiment 351, 91405 Orsay Cedex, France*
[2]*Laboratoire des Collisions Atomiques et Moléculaires, Université Paris-Sud, UMR 8625, Bâtiment 351, 91405 Orsay Cedex, France*
[3]*Department of Applied Physics, Chalmers/Göteborg University, S-41296 Göteborg, Sweden*
(Received 11 February 2008; published 1 May 2008)

We present a theoretical study of the energies, lifetimes, wave functions, and decay paths of the excited electronic states in corral structures formed by Cu adatoms on the Cu(111) surface. Three different corrals with 35, 48, and 70 Cu adatoms have been studied within a joint approach including the density functional theory and wave packet propagation. Confinement of the electronic surface state inside the corral structure leads to the formation of well-defined resonances in the density of electronic states. Particular emphasis is given in the present work to the role of excited electronic states localized on the ring of Cu adatoms forming the corral. While never discussed in the past for corral structures, these states are equivalent to the one-dimensional *sp* band of Cu atomic chains assembled on the Cu(111) surface that has been recently studied thoroughly. The coupling between the confined surface state resonances and the *sp* state localized on the Cu ring have been studied in detail. It is shown that the *sp* state localized on the corral wall appears as a strong perturbation in the spectrum of confined states.

DOI: 10.1103/PhysRevB.77.205403 PACS number(s): 73.20.At, 73.20.Hb, 73.22.−f, 68.37.Ef

I. INTRODUCTION

The development of scanning tunneling microscopy (STM) offers a unique opportunity for the observation and the manipulation of matter on the atomic scale.[1] The quantum corrals represent spectacular and probably the most studied artificial structure built atom by atom on a metal surface.[2–6] Starting from the very first observations of quantum corrals, many experimental and theoretical works were devoted to or have exploited the role of the quantum corrals in the two-dimensional (2D) confinement of the surface state electrons. Indeed, because of the presence of a projected band gap, the electrons in the surface state at the close-packed faces of noble metals are bound to the metal-vacuum interface and move quasifreely parallel to the surface.[7] The ring of adatoms forming the corral reflects the surface state electrons, leading to their confinement inside the corral. It has been shown that this confinement effect is responsible for the quantization of the 2D-surface state continuum and the appearance of the well-defined resonances in the electronic density of states.[2–6,8–11] The corresponding standing-wave patterns of the electronic density inside the quantum corral have been experimentally observed.[2,3] The reflection of the surface state electrons by the boundary of the artificially built structure has also been shown to lead to quantum mirages, including the image of the Kondo resonance in the case of elliptic corral.[5,10,12–15]

From the theoretical point of view, the description of the surface state quantization phenomena in the corral structures is analogous to that in the case of vacancy and adatom islands.[16–24] Namely, the states localized inside the nanostructure are quasistationary (resonances) with their energies well described within the particle-in-a-box picture. The confined states decay via one-electron scattering at the boundaries. Possible decay channels comprise electron transfer into the bulk states and into the surface state continuum outside the structure. Many-body decay processes (electron-electron and electron-phonon scattering) also contribute to the finite lifetime of the confined states.[22,25,26] As follows from the above discussion, the corral wall has been considered until now only through its confining action on the surface state electrons. To the best of our knowledge, the possibility of specific electronic states localized on the chain of adatoms forming the corral was not investigated.

The possibility of having electronic states localized on the corral wall is strongly suggested by a series of recent STM studies that revealed excited electronic states localized on individual metal adatoms as well as on linear and kicked adatom chains supported on metal surfaces.[27–34] For example, in the case of a Cu adatom on Cu(111), the Cu 4*s* and 4*p* atomic orbitals, which are at the origin of the *sp* conduction band in bulk Cu, hybridize on an adatom and lead to an unoccupied resonance located a few eV above the Fermi level.[31] In the case of atomic chains on the surface, the *sp* resonances located at neighboring adatoms are coupled. For an infinite Cu chain, a one-dimensional (1D) *sp* band of excited electronic states appears. It corresponds to an electron propagating along the chain and that is partially decoupled from the bulk because of the projected band gap of Cu(111). On a finite chain, confinement of the 1D *sp* band leads to quantized 1D states delocalized over the chain. Comparison between the STM data and *ab initio* calculations[31,35] fully supports the above picture. Similarly, the appearance of a 1D band of specific states localized on atomic chains has been reported for Au and Pd atomic chains on the NiAl(110) surface.[27–30] *Ab initio* density functional calculations of the Au-chain/NiAl(110) system confirmed the *sp* character of the 1D band of excited electronic states and the role of the surface projected band gap has been underlined.[36] The partial decoupling of the chain localized states from the metal bulk continuum explains the success of the tight binding modeling of the STM data by only considering the chain atoms.[31,32] This is a remarkable result since one would naturally expect that *sp* states localized on an adsorbate would couple as strongly with the substrate atoms as with the adatoms in the chain and finally get integrated into the substrate *sp* conduction band.

Recently, we have studied the energy, lifetime, and decay paths of the 1D *sp* band localized on an infinite Cu wire on Cu(111).[37] The energies and widths of the 1D *sp* band states are found to be in good agreement with the experimental data of Fölsch *et al.*[31] The calculated lifetimes of the 1D *sp* band states allowed us to specify the extent to which the 1D *sp* band on the wire can be considered as independent of the Cu substrate. Actually, an atomic Cu wire supported on a Cu(111) surface can be considered as a short wire, along which electrons can travel over up to 12 Å before leaving the wire.[37]

In the light of the results described above, let us consider that an atom adsorbed on a metal induces a resonance in the density of unoccupied electronic states above the Fermi level. This resonance corresponds to the transient trapping of an excited electron at the adsorbate. If a ring of such atoms is built into a corral, the states localized on the individual adatoms will interact together forming electronic states delocalized along the corral wall. Another way of coming to the same conclusion is to look at the corral wall as a Cu atomic chain bent into a circle. Obviously, the 1D *sp* band of excited states localized on the chain will be transformed into a band of circular electronic states. Therefore, for such a corral, one can expect to observe two different kinds of quasistationary states: (i) confined surface states localized inside the corral (thoroughly discussed in the literature on quantum corrals) and (ii) resonances localized on the metal adatoms forming the corral.

The present paper is devoted to a theoretical study of the electronic properties of Cu corrals on a Cu(111) surface. Three different corral sizes were considered (wall made of 35, 48, and 70 adatoms). The electronic states in this system are investigated with a joint wave packet propagation (WPP) and density functional theory (DFT) approach. The energy, lifetime, decay paths, and wave functions of the corral specific electronic states were obtained. We show that, within a certain energy range, the quasistationary states resulting from the confinement of the surface state electron inside the corral strongly interact with the circular *sp* states localized on the corral wall. Basically, the presence of the *sp* state strongly perturbs the spectrum of the confined surface states. The paper is organized in the following manner. Section II introduces the theoretical methods employed. We present and discuss the results obtained in Sec. III. We end with some conclusions in Sec. IV.

II. THEORETICAL METHODS

The system under study is schematically presented in Fig. 1. The corral is made of Cu adatoms placed along a large radius circle on a Cu(111) surface. It corresponds to a supported Cu wire that has been bent into a perfect circle: the distance between the Cu adatoms along the circle is equal to the bulk Cu-Cu distance and the adsorption height of the circle is the same as that of an infinite Cu wire on Cu(111). The radius R of the corral is equal to $R=\frac{N_a \ell}{2\pi}$, where N_a is the number of adatoms forming the corral and ℓ is the period of the atomic wire, i.e., the bulk distance between two Cu atoms: $\ell=a/\sqrt{2}$ ($a=3.59$ Å, lattice constant of Cu). Following

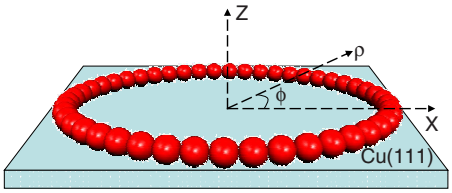

FIG. 1. (Color online) Schematic representation of the system under study: a Cu corral supported on a Cu(111) surface. The cylindrical coordinate system $\mathbf{r}=(\rho,\phi,z)$ is such that the origin of coordinates is placed at the geometrical center of the atomic ring forming the corral and the z axis is normal to the surface.

the system symmetry, we used a cylindrical set of coordinates for the active electron $\mathbf{r}=(\rho,\phi,z)$, with the z axis normal to the surface and going through the corral center (see Fig. 1). This is an idealized structure since the constitutive adatoms are not at the proper adsorption sites. Such a choice greatly simplifies the theoretical study and we think that a more realistic enclosure, which is made, e.g., of short straight atomic chains, would exhibit the same physical effects as discussed here. Similarly, the present qualitative results should also hold for a larger interatomic distance between the adatoms forming the corral wall, as was used in the earlier corral studies. In both cases, only the actual energy position of the quasistationary states would change.

Our approach is a joint DFT-WPP approach similar to that used earlier for the study of Cu adatoms on Cu(111).[38–40] It consists in (i) modeling the interaction potential of the active electron with the system (surface+corral) using data from an earlier DFT study of supported Cu wires and (ii) WPP study of the time evolution of the active electron in this interaction potential that yields the characteristics of the quasistationary states in the system.

The interaction potential between the active electron and the entire system is obtained as the sum of the electron interaction potential with the clean Cu(111) surface $V_s(z)$ and the potential induced by the Cu adatoms of the corral wall ΔV^c. The model electron-clean surface interaction potential has been taken in the form proposed by Chulkov *et al.*[41] on the basis of their *ab initio* studies. This is a one-dimensional analytic potential that very accurately reproduces the electronic structure of Cu(111) at the $\bar{\Gamma}$ point. The potential only depends on the electron-surface distance z and a free electron motion parallel to the surface is assumed.

The corral-induced potential ΔV^c has not been directly computed but modeled from a bending transformation (see below) of the DFT results of our earlier study on supported Cu wires on Cu(111).[37] The DFT calculations used a plane-wave pseudopotential method as implemented in the VASP code[42] in a supercell geometry (four Cu layers and four "vacuum layers"). The Kleinman-Bylander-type pseudopotentials[43] V_{PP} were used to describe electron-Cu core interactions (see details in Refs. 37 and 40). The wire-induced exchange-correlation potential ΔV^w_{XC} and the wire-induced electron density Δn^w were obtained from the difference between the corresponding quantities in the calculation of the clean Cu(111) case and of the supported wire case. The supercell was large enough so that ΔV^w_{XC} and Δn^w are

well localized inside the cell for both the direction perpendicular to the surface and the direction parallel to the surface and perpendicular to the wire. Then, the corral-induced electron density Δn^c is calculated by considering the transformation in which a finite length atomic wire is bent into a full circle and by assuming that the electron density is transformed accordingly keeping the density constant in an infinitesimal volume, i.e., $\Delta n^c(\rho,\phi,z)=\Delta n^w(x',y',z')\frac{R}{\rho}$, where (x',y',z') are the electron Cartesian coordinates in the atomic wire case (x' is along the wire, z' is perpendicular to the surface, and the origin is centered on one of the wire atoms). The coordinate correspondence is such that $z=z'$, $\rho=R+y'$, and $\phi=\frac{x'}{R}$. The induced density for the corral Δn^c is periodic in ϕ, in the same way as the induced density Δn^w is periodic along the atomic wire. The period is $\Delta\phi=\frac{2\pi}{N_a}$. The corral-induced Hartree potential ΔV_H^c is then obtained from $\Delta n^c(\rho,\phi,z)$ by solving Poisson's equation. Such a procedure is justified by the large corral radii we are considering ($R=26.72a_0$, $36.65a_0$, and $53.44a_0$ for 35, 48, and 70 atoms, respectively), much larger than the spread of the electron density around the Cu atomic wire. The corral-induced exchange-correlation part of the potential ΔV_{XC}^c was obtained from its equivalent for the atomic wire via $\Delta V_{XC}^c(\rho,\phi,z)=\Delta V_{XC}^w(x',y',z')$. The ion cores in the corral were represented by the Kleinman-Bylander pseudopotential identical to the one used in the DFT study $V_{\text{ion}}=\Sigma_j V_{\text{PP}}(\mathbf{r}-\mathbf{r}_j)$, where the summation runs over all the Cu adatoms forming the corral. As a result, the total corral-induced potential ΔV^c was calculated from $\Delta V^c=\Delta V_{XC}^c+\Delta V_H^c+V_{\text{ion}}$. The interaction potential between the active electron and the entire system (surface+corral) is

$$V=V_s(z)+\Delta V_H^c(\rho,\phi,z)+\Delta V_{XC}^c(\rho,\phi,z)+V_{\text{ion}}(\rho,\phi,z). \quad (1)$$

This total interaction potential is then used in a WPP calculation that studies the one-electron dynamics in the system to get the characteristics of the quasistationary states. Only a brief outline of this method is given below; further details on the WPP approach can be found in Refs. 25 and 44. The WPP approach basically consists of solving the time-dependent Schrödinger equation on a grid of points in the cylindrical coordinates defined above. Because of the periodicity of the problem in the ϕ coordinate, the wave function of the active electron $\Psi(\mathbf{r},t)$ is taken as a Bloch function $\Psi(\mathbf{r},t)=e^{im\phi}\psi^m(\mathbf{r},t)$, where m is the magnetic quantum number and ψ^m is periodic in ϕ with the period $\Delta\phi$. Here, m varies within the $0\leqslant m<N_a/2$ range, $\pm|m|$ states being degenerate. The time evolution of ψ^m is given by

$$i\frac{\partial\psi^m(\mathbf{r},t)}{\partial t}=H^m\psi^m(\mathbf{r},t), \quad (2)$$

with the initial condition $\psi^m(\mathbf{r},t=0)\equiv\psi_{init}^m(\mathbf{r})$. The Hamiltonian in cylindrical coordinates reads

$$H^m=-\frac{1}{2}\frac{\partial^2}{\partial z^2}-\frac{1}{2\rho}\frac{\partial}{\partial\rho}\rho\frac{\partial}{\partial\rho}-\frac{1}{2\rho^2}\left[\frac{\partial}{\partial\phi}+im\right]^2+V(\rho,\phi,z)+V_{\text{opt}}(\rho,z), \quad (3)$$

where $V(\rho,\phi,z)$ is the electron potential given in Eq. (1). $V_{\text{opt}}(\rho,z)$ is an absorbing potential[45] introduced to impose outgoing wave boundary conditions (in the ρ and z coordinates) and thus to avoid artificial reflections of the wave packet at the boundaries of the calculation box.

In practice, the time-dependent wave packet, $\psi^m(\mathbf{r},t)$, is represented on a finite size mesh in cylindrical coordinates comprising ($N_\rho=1000$, $N_\phi=24$, $N_z=768$) points in ρ,ϕ, and z coordinates, respectively. The N_ϕ points of the mesh span a period of the structure $\Delta\phi$ (one corral Cu adatom per period). The numerical solution of Eq. (2) is obtained via short time propagation, involving the split operator approximation.[46] The propagation step was typically set to $dt=0.05$ a.u. The Fourier-grid pseudospectral method[47] was used for the calculation of the z and ϕ spatial derivatives in the propagator, whereas a Cayley transform[48] associated with a finite difference scheme and coordinate mapping was used for the ρ part.[49]

From the time-dependent electron wave function, $\psi^m(\mathbf{r},t)$, and the corresponding survival amplitude $A(t)$,

$$A(t)=\langle\psi_{init}^m(\mathbf{r})|\psi^m(\mathbf{r},t)\rangle, \quad (4)$$

the projected density of (electronic) states (PDOS) onto the initial state is obtained via time-to-energy transform,

$$n(\omega)=\frac{1}{\pi}\text{Re}\left\{\int_0^\infty e^{i\omega t}A(t)dt\right\}. \quad (5)$$

The various resonances in the system can be recognized in the PDOS to the extent that they have a significant overlap with the initial state ψ_{init}^m, so that a clever choice of the initial state simplifies the convergent extraction of the energies E, widths Γ, and wave functions of the quasistationary (decaying) states of the system. In the present work, E and Γ are obtained from a fit of the survival amplitude $A(t)$ to a sum of complex exponential functions (see Ref. 14). The resonance wave function at the energy ω can be extracted from the time-dependent wave packet as follows:

$$\psi_\omega^m(\mathbf{r})=\int_0^\infty e^{i\omega t}\psi^m(\mathbf{r},t)dt. \quad (6)$$

Since the WPP calculation is monoelectronic, the width Γ of the resonances obtained in the above calculation is equal to their decay rate by one-electron energy-conserving transfer into the bulk and surface electronic states of Cu(111) substrate. Multielectron transitions can also contribute to the quasistationary state decay; this point is further discussed below.

The main objective of this work is to search for two different types of quasistationary states associated with the quantum corral structure: (i) the *sp* state localized on the Cu adatoms forming the corral wall and equivalent to the 1D *sp* band observed on Cu wires and (ii) the states coming from the surface state confinement inside the corral. The WPP procedure yields the density of states projected on the initial wave function, and so, for locating a particular kind of states, it is advisable to start with a well-chosen initial condition that can be thought to have a significant overlap with the

states to be studied. Thus, to locate the *sp* state, we have performed WPP calculations with an initial wave packet of the type

$$\psi_{init}^{m}(\mathbf{r}) = \psi_{p_z}(\rho,\phi,z) = ze^{-s^2/b}, \tag{7}$$

where s is the distance between the electron and the corral atom, which is inside the calculation box. Thus, $\psi_{init}^{m}(\mathbf{r})$ is a p_z-type orbital centered on the atoms of the corral. We took $b=12.5a_0^2$ in Eq. (7), known to be a good estimate of the *sp* state extent from our earlier study on Cu wires.[37] The confined surface states within a given m-symmetry subspace have been searched using $\psi_{init}^{m}(\mathbf{r})=\psi_{m,j}(\rho,\phi,z)$ initial wave functions, where

$$\psi_{m,j}(\rho,\phi,z) = \begin{cases} 0, & \rho > R, \\ J_m(k_{m,j}\rho)\chi(z), & \rho \leqslant R, \end{cases} \tag{8}$$

where J_m is the mth order Bessel function, $k_{m,j}=Z_{m,j}/R$, R is the radius of the corral, and $Z_{m,j}$ is the jth zero of J_m. The dependence of $\psi_{m,j}$ on the z coordinate perpendicular to the surface is given by the wave function $\chi(z)$ of the surface state for the clean Cu(111). A wave function given by Eq. (8) is a simple estimate corresponding to the surface state quantized inside the corral with a perfectly reflecting circular boundary.

III. RESULTS

A. Projected density of states and wave functions

A first set of WPP calculations was performed using initial wave functions given by Eq. (8). For each given initial state $\psi_{m,j}(\rho,\phi,z)$, the corresponding PDOS (not shown here) is dominated by a very small number of peaks. These peaks correspond to quasistationary states (resonances) with a finite lifetime. We label the various resonances appearing in this set of calculations as (m,p) states: m is according to their symmetry and p is an index following the increasing energy order of the various states. For the lowest j initial functions, only one resonance is present in the PDOS, so that it can be directly assigned to a confined surface state and there is one to one correspondence: $p=j$. For the higher j initial functions, several peaks are present in the PDOS. A one to one correspondence cannot be made between the (m,p) resonances in the system and the various $\psi_{m,j}$ initial states. Nevertheless, we can stress that all the (m,p) resonances in this system can be generated using $\psi_{m,j}$ initial functions. It is noteworthy that for a given m, there also exist states with a larger number of angular nodes. These states are much higher in energy and have not been studied here.

We now turn to the detailed discussion of the results obtained with an initial wave function of the *sp* type [Eq. (7)]. Figure 2 shows the corresponding PDOS for the $m=0$ symmetry for the three systems studied (35, 48, and 70 atoms). Vertical lines labeled (m,p) in Fig. 2 represent the WPP results for the energies of the various resonances of the system obtained with $\psi_{m,j}(\rho,\phi,z)$ initial wave functions. A detailed discussion of the energy spectrum of the (m,p) states is presented later in the text.

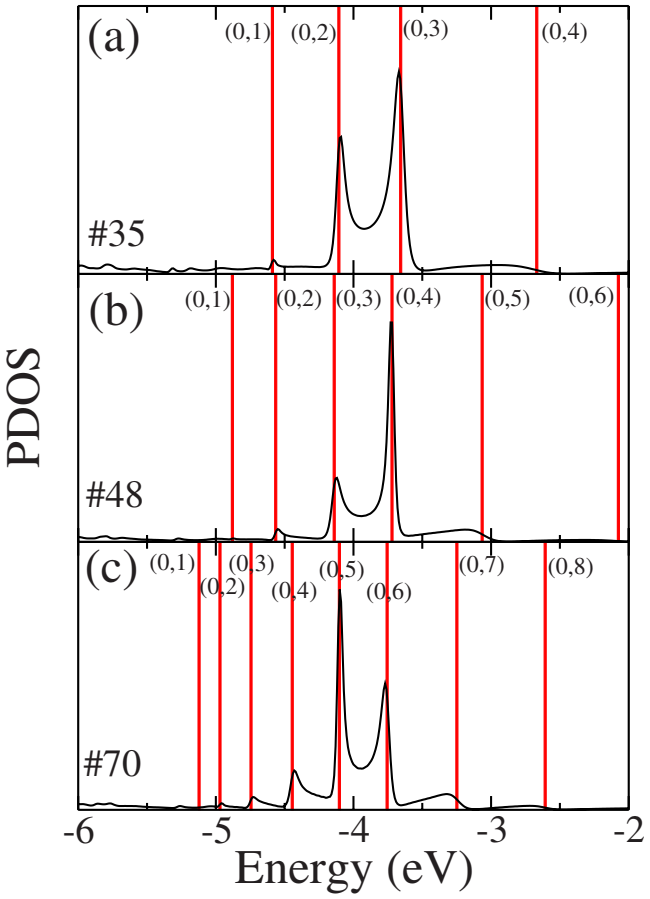

FIG. 2. (Color online) Projected density of states (PDOS) obtained in the $m=0$ symmetry using the initial wave function of *sp* type [Eq. (7), see text for details] for the corrals with (a) 35 atoms ($R=26.72a_0$), (b) 48 atoms ($R=36.65a_0$), and (c) 70 atoms ($R=53.44a_0$). Results are shown as functions of the electron energy measured with respect to the vacuum level. The vertical red lines show the energies of the various resonances in the system, labeled by (m,p).

In Fig. 2, the PDOS does not contain any new peak compared to the resonance spectrum that we obtained with the $\psi_{m,j}(\rho,\phi,z)$ initial wave functions. Indeed, there is not a single peak that we could directly assign to the *sp* state, although the initial state is *a priori* perfectly adapted to locate a *sp* resonance localized on the corral wall. Actually, for each corral, the PDOS exhibits a series of peaks located at the energies of certain resonances, but not at all of them. Furthermore, analysis of the time dependence of the wave packet survival with an *sp* initial wave function yields energies and widths of the resonances that perfectly match those obtained using quantized surface states as initial states for the time propagation. No other resonance appears. This is quite different from the equivalent calculations performed for a single Cu adatom[38] or for an infinite supported Cu wire[37] where specific peaks attributed to the *sp* state appear in the PDOS. The *sp* resonance of the single Cu adatom has a width around 0.5 eV and it is located at an energy of −2.25 eV (with respect to vacuum).[38] For a supported Cu wire, the energy of the 1D *sp* band at the band bottom is at −4.07 eV with respect to vacuum and the corresponding

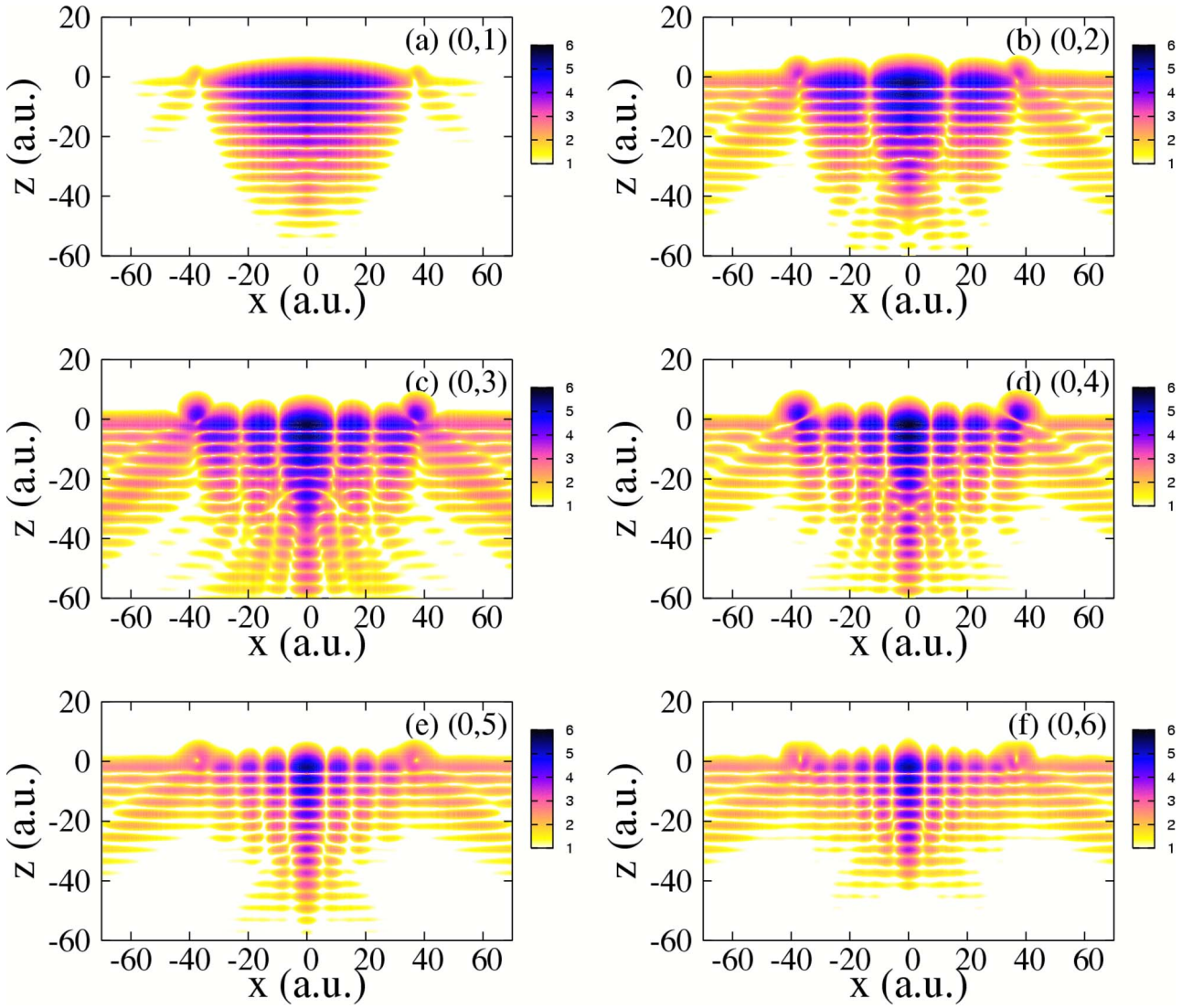

FIG. 3. (Color online) Contour plot of the logarithm of the electron density (arbitrary units) for different resonances in the case of the corral with 48 atoms. The density is shown in the (x,z) plane perpendicular to the Cu surface that contains the center of the corral and that goes through the center of two Cu atoms on opposite sides of the corral. x is the coordinate parallel to the surface and z is the coordinate perpendicular to the surface. z is positive in vacuum and $z=0$ corresponds to the center of the corral atoms. x and z are in a.u. The six different panels of the figure correspond to (a) ($m=0$, $p=1$), (b) (0,2), (c) (0,3), (d) (0,4), (e) (0,5), and (f) (0,6) corral states. The color code is explained in the inset.

width is 0.32 eV.[37] Since the corral is obtained via bending of a Cu wire, one would expect the $m=0$ sp state in the corral to have an energy close to that of the 1D sp band bottom of the supported wire. Although no specific peak appears in this region, for the three corrals that were studied, the strongest peaks in the PDOS correspond to the energy region where the sp state is expected.

To get further insight into the character of the various (m,p) resonances in this system, we computed the corresponding wave functions. Figure 3 presents the electron density for the ($m=0$, $p=1-6$) states for the corral made of 48 atoms. The electron density is shown in the (x,z) plane, where z is the coordinate perpendicular to the surface (positive in vacuum) and x is one of the coordinates parallel to the surface (see Fig. 1). The origin of coordinates is at the center of the corral. The x axis goes through the center of the two opposite atoms of the corral which are located at $\rho=R=36.6a_0$, i.e., they appear in the figure at $z=0$ and $x=\pm 36.6a_0$.

As a first feature, all states exhibit a very large electron density inside the corral. This inner electron density shows the z dependence characteristic of the surface state localized on the clean Cu(111) surface: exponentially decaying oscillations into the metal and an exponential tail in the vacuum side. The radial dependence of the electron density exhibits a well marked nodal structure that varies from one state to the other. Thus, the overall appearance of the wave functions of the resonances corresponds well to what is expected for quantized states formed by confinement of the surface state. As for an sp component in the resonant wave functions, one can recall that in the case of a single adatom or in the case of Cu wires on Cu(111),[31,37,38] the sp state is associated with an

electron density located in vacuum slightly above the Cu adatom or wire. This shape is a direct consequence of the *sp* hybrization; similar situations have been encountered and illustrated in many atom-metal surface interacting systems.[36,50–53] In Fig. 3, the (0,3) and (0,4) states exhibit a significant electron density in this region above the Cu adatom (the Cu adatom center is in the $z=0$ plane), whereas the other (m,p) states exhibit a weaker *sp* component. This is perfectly consistent with the PDOS in Fig. 2(b), which reveals a significant *sp* component concentrated in the (0,3) and (0,4) states.

Let us look at the wave functions one by one in more detail. The radial structure of the electron density of the (0,1) resonance corresponds well to the trial particle-in-a-box function in Eq. (8) with a radial part given by a Bessel function $J_0(k_{0,1}\rho)$ vanishing at the corral wall. Similarly, the (0,2) state appears as the second quantized state coming from the confinement of the surface state, with a node on the corral wall and another node at a finite radius. At first glance, the case of the (0,5) and (0,6) states is similar. However, careful examination of their radial nodal structures shows that they correspond to the fourth and fifth quantized levels, respectively, although they are the fifth and sixth resonances following the increasing energy order. So the lowest lying and highest resonances do qualitatively correspond to confined surface states; however, there is a jump of one unit in their labeling, i.e., compared to a simple confined surface state case, an extra state is present in the resonance spectrum.

Obviously, this extra state has to be the *sp* state. However, it is not easy in the present system to clearly assign one of the resonances to the *sp* state. As seen in Fig. 2, the *sp* character is spread over several (m,p) states. Qualitatively, if we consider the *sp* state and quantized surface states defined independently, the *sp* state is located around −4 eV and couples very efficiently with the confined surface states in this energy range. As a result, a group of levels with a mixed character appear in the −4 eV energy range [these are precisely the (0,3) and (0,4) states in the corral with 48 atoms]. The confined states far below [the (0,1) and (0,2) states] or far above [the (0,5) and (0,6) states] from the *sp* state are only weakly perturbed. Observe also that the spread of the *sp* character over the (m,p) states varies with the corral radius (see Fig. 2). Indeed, as the corral radius increases, the density of the quantized surface states increases, leading to a larger number of confined states strongly mixed with the *sp* state.

Besides the information on the wave functions of the quasistationary electronic states formed by the Cu corral on Cu(111), Fig. 3 reveals additional information about the resonance decay channels. Indeed, because of the scattering at the Cu adatoms forming the corral, the corral localized states can decay by energy-conserving one-electron transitions into substrate states. Thus, in Fig. 3, the decay appears as an outgoing flux of electrons originating from the corral wall. The electron escapes both in the surface state continuum (parallel to the surface with a maximum at slightly negative z values) and into three-dimensional (3D)-bulk states. The (0,1) state is low in energy and has a very small width (see below), so that the outgoing flux appears very weak in Fig. 3. Note that the decay into the 3D-bulk states starts at a finite angle from the surface normal, as a consequence of the

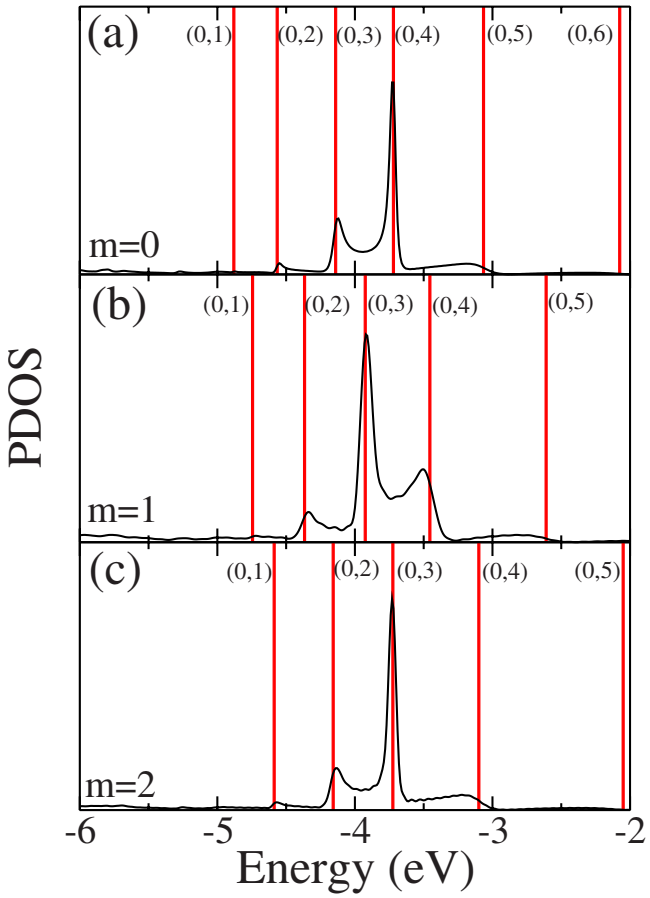

FIG. 4. (Color online) PDOS obtained using the initial wave function of *sp* type [Eq. (7), see text for details] for a corral with 48 atoms. Results are shown as a function of electron energy measured with respect to the vacuum level. The vertical lines show the energies of the resonances in the system labeled by (m,p). Panels (a), (b), and (c) correspond to $m=0$, 1, and 2 symmetries, respectively.

Cu(111) surface projected band gap that forbids an outgoing flux normal to the surface [see a discussion of a similar case for alkali/Cu(111) (Refs. 51–53)]. One can also note that the decay into 3D-bulk states of the confined states only occurs outward, whereas the states with a significant *sp* character also exhibit an inward decay into the 3D-bulk states, as expected for an *sp* state located on the corral wall. This inward decay flux interferes with the evanescent tail of the surface state inside the bulk leading to a complex structure in the electron density around $z=-40a_0$. This interference is particularly visible in the (0,3) and (0,4) states, again pointing at the strong *sp* character of these two states. In either situation, the decay into the surface state continuum is the main decay channel of the corral resonances as follows from the high relative intensity of the corresponding flux. The same result has been observed for the 1D *sp* band of the Cu wire on the Cu(111) surface.[37]

We have also carried out calculations for the corral of 48 atoms with different values of the magnetic quantum number $m=0$, 1, and 2. The PDOS obtained in the case of an *sp*-type initial wave function [Eq. (7)] is presented in Fig. 4 for the $m=0$, 1, and 2 symmetries [panels (a), (b), and (c), respectively]. The results are very similar to those found in the *m*

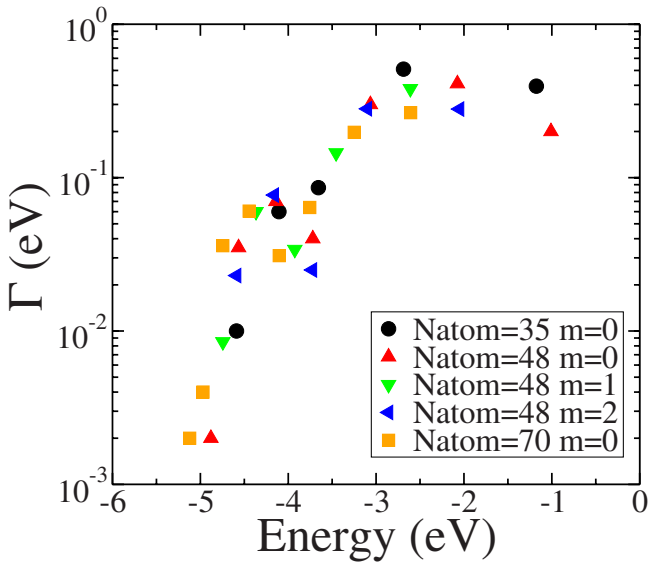

FIG. 5. (Color online) Width of all the confined surface states (m,p) that have been studied as a function of their energy with respect to vacuum (see Figs. 2 and 4). Black circles: $(0,p)$ states in the corral with 35 atoms. Yellow squares: $(0,p)$ states in the corral with 70 atoms. Red triangles up: $(0,p)$ states; green triangles down: $(1,p)$ states; and blue triangles left: $(2,p)$ states in the corral with 48 atoms.

$=0$ symmetry. As expected, the energy of the (m,p) resonances shifts upward with increasing angular momentum m. In contrast, the envelope of the spectrum (the part of sp character in the resonances) does not shift much with m. This is not surprising for an sp state which should exhibit a very small energy shift at low m's due to the large corral radius. As a result, the index p of the quantized surface state located at the maximum of the sp character shifts from 4 to 3 when m is increased.

B. Lifetime of the resonances

The analysis of the width (Γ) of the (m,p) resonances reveals interesting information on the system dynamics. In particular, the width (inverse of the one-electron lifetime $\tau=1/\Gamma$) reflects the strong perturbation of the confined surface states which are close in energy to the sp state of the Cu adatoms on the corral wall. Figure 5 shows the width of all the (m,p) states that we studied as a function of their energy with respect to vacuum. It appears that the results roughly fall on a single curve, i.e., that the energy of the resonance is the main parameter governing its lifetime (see also Refs. 20 and 54). Consistently, with previous studies on confined structures at surfaces,[3,8–11,20,22,24,54] when the energy of the (m,p) state approaches the surface state band bottom $[E_0=-5.33$ eV for clean Cu(111)], the corresponding width becomes smaller (larger lifetime). At larger energies, the width tends to ~0.5 eV. This general trend of variation of the level width can be understood as follows: an electron in the confined state can be seen as moving freely inside the corral and, from time to time, hitting the wall where it has a finite probability of escaping from the corral. The confined state decay rate can then be approximated by the product of an attempt frequency by a transition probability at the corral wall, the latter dominating the energy dependence. One can expect the corral wall transparency to increase when the electron energy parallel to the surface increases, enhancing the state decay. However, the most interesting feature of the variation of the width is the oscillation appearing for energies close to −4 eV. The (m,p) states in this energy range correspond to a mixture of a confined surface state and the sp resonance localized on the Cu atom ring. Then, the decay of the (m,p) states depends on the interference between the decay of their two components, leading to the Fano profile[55] structure seen in Fig. 5.

At this stage, one can stress that the decay rate of the quantized states obtained from WPP calculations and shown in Fig. 5 corresponds to one-electron energy-conserving transitions into the surface state continuum and the 3D-bulk states. However, an excited electron can also decay via many-body inelastic interactions with the bulk electrons and phonons.[25,26] We did not attempt to evaluate this contribution. However, its order of magnitude can be discussed based on similar systems. For example, the many-body inelastic contribution to the excited state decay for the sp state in alkali/Cu(111) systems was computed to be in the 20 meV range.[56] For a Cu adatom, the many-body contribution can be expected to be smaller since the sp state is closer to the Fermi level than for the alkalis. These estimates are much smaller than the typical one-electron width obtained for the sp state of a single adatom[38] or of a Cu wire,[37] which is in the few hundred meV range. For the quantized surface states, the many-body decay rate can be estimated from that of the surface state on a clean Cu(111) surface. At the bottom of the Cu(111) surface state continuum, the width due to electron-electron and electron-phonon interactions is in the 20 meV range both from experimental and theoretical studies.[57–59] At higher energies, the surface state lifetime on Cu(111) is mainly attributed to inelastic electron-electron interactions and it has been measured from the analysis of interference patterns.[60] Around 1 eV above the Fermi level, an important region in the present discussion, the surface state width is around 40 meV and it goes up with energy roughly like $(E-E_F)^{-2}$ [see also Ref. 25]. This is significant compared to the present one-electron width of the (m,p) states (see Fig. 5); however, this should not alter the present discussion about the evidence for the perturbation induced by the sp state in the quantized surface state levels.

C. Analysis of the energy spectrum of the resonances

The analysis of the energies of the corral states reveals further information on the role of the sp resonance and on how the presence of the "extra" state induces changes among the quantized states coming from the confinement of the surface state. To this end, let us compare the actual energies of the corral states as obtained in the WPP calculation to those predicted by a simple particle-in-a-box model. For a 2D circular corral with a perfectly reflecting boundary at radius R_{eff}, the quantization energies of the confined states, $E_{m,p}^{model}$, can be estimated from

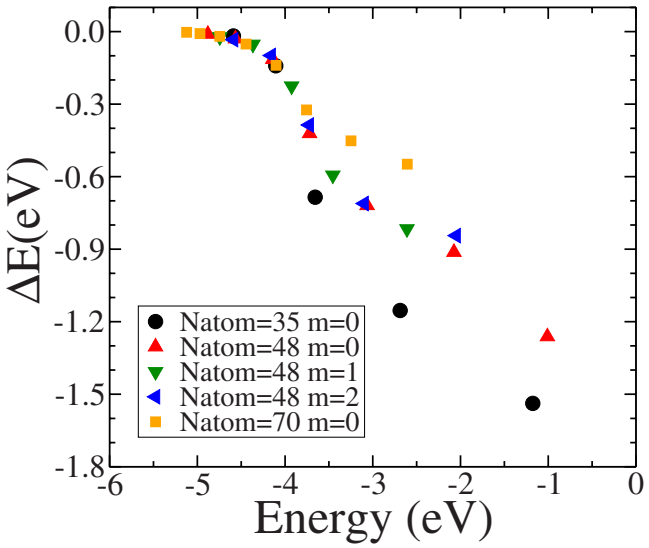

FIG. 6. (Color online) Difference between the energies of the $(m=0,p)$ corral states obtained in the WPP calculation and in the particle-in-a-box model. The energy difference is expressed as a function of the energy in the WPP calculation. Results for a corral with 35 atoms (black circles), 48 atoms (red triangles), and 70 atoms (yellow squares) are shown.

$$E_{m,p}^{model} = E_0 + \frac{Z_{m,p}^2}{2R_{eff}^2 m_{\bar{e}}} + \langle \psi_{m,p} | \Delta V_{loc}^c | \psi_{m,p} \rangle, \tag{9}$$

where E_0 is the energy of the surface state continuum on the clean Cu(111) surface at the $\bar{\Gamma}$ point ($E_0=-5.33$ eV), $Z_{m,p}$ is the pth zero of the Bessel function of order m (different from zero for $|m| \geq 1$), and R_{eff} is the effective radius where confinement occurs. Similarly to other works,[20,24] it has been assumed that confinement occurs on the inner edge of the Cu corral atoms and R_{eff} was taken equal to $R-\ell/2$, where R is the corral radius defined above and ℓ the Cu-Cu distance along the corral wall. $m_{\bar{e}}$ is the electron effective mass in the surface state continuum. In the present study, using the model potential from Ref. 41, $m_{\bar{e}}$ is equal to the free electron mass. Since the corral-induced potential ΔV^c is not exactly zero inside the corral, the particle-in-a-box prediction has to be corrected for this background potential. It has been evaluated by simply shifting the energies of the confined states by the mean value of the local part of the corral-induced potential, $\Delta V_{loc}^c(\rho,\phi,z)=\Delta V_H^c(\rho,\phi,z)+\Delta V_{XC}^c(\rho,\phi,z)$, over the initial state $\psi_{m,p}$ given by Eq. (8). The latter corresponds to the wave functions of the states confined on the flat surface inside the corral.

Figure 6 shows the difference $(E_{m,p}^{WPP}-E_{m,p}^{model})$ between the WPP results and the model prediction [Eq. (9)] for the energies of the $m=0$ states. Results are shown as a function of the corral state energy obtained with WPP. The simple particle-in-a-box model appears excellent for the lowest lying states. However, the agreement rapidly worsens as the energy is increased. The disagreement starts sharply around −4 eV. This behavior is not surprising in view of the discussion of the character of the states based on their wave functions as was presented in Sec. III A of this paper. In the region around −4 eV, an extra state appears in the spectrum of confined states leading to the breakdown of the particle-in-a-box model. However, pure confined states do reappear in the upper part of the spectrum.

This aspect of the departure of the confined state energy from the particle-in-a-box prediction has been analyzed along the following lines, which is inspired from the analysis of atomic and molecular spectra.[61,62] Indeed, in atomic and molecular spectra, it often occurs that a Rydberg series of states is perturbed by an extra state coming from, e.g., a higher lying series. The perturbation of the Rydberg spectrum is then analyzed in terms of an extra phase or extra quantum defect introduced by the so-called "interloper state."[61,62] A similar analysis can be performed here. In the case of a free 2D wave of m symmetry confined in a circular box, the radial part of the confined wave is equal to a Bessel function, $J_m(k\rho)$, which vanishes on the edge of the confining surface at $\rho=R_{eff}=R-\ell/2$, i.e.,

$$k_{m,p}^{model} = \frac{Z_{m,p}}{R-\ell/2}. \tag{10}$$

From the WPP result $E_{m,p}^{WPP}$ for the energy of the (m,p) corral state, one can obtain the corresponding effective momentum,

$$k_{m,p}^{WPP} = \sqrt{2(E_{m,p}^{WPP} - E_0 - \langle \psi_{m,p} | \Delta V_{loc}^c | \psi_{m,p} \rangle)} \tag{11}$$

[cf. Eq. (9)]. Note that the energy term due to ΔV^c, the nonvanishing potential inside the corral, has been evaluated using confined wave functions, which is not appropriate for the higher lying (m,p) states. This energy term, of the order of a fraction of an eV, varies with the corral radius; however, it only very weakly depends on the m and p indices, so that Eq. (11) is a good approximation for the present analysis.

The difference in energy or in momentum of the corral state as compared to the particle-in-a-box model can then be reexpressed as an additional phase appearing because of the scattering at the corral wall and equal to

$$\delta\varphi = R_{eff}(k_{m,p}^{WPP} - k_{m,p}^{model}). \tag{12}$$

This phase shift expresses the difference between a perfectly reflecting wall and an actual corral made of Cu adatoms.

Figure 7 presents the $\delta\varphi$ phase shift as a function of the energy for all the (m,p) states that we studied. It is remarkable that all the phase shifts extracted for different m symmetries and for different corral radii roughly fall on a single curve. $\delta\varphi$ presents a sharp variation around ~−4 eV. The phase shift is small at small energy consistently with the very good agreement between the energies of the particle-in-a-box states and those obtained in the present WPP calculation. In the region of −4 eV, the phase shift sharply increases by a little more than 2 rad at higher energies. This sharp increase is attributed to the perturbation introduced by the *sp* state. Usually in such a phase analysis, a sharp increase in the phase shift by π radians indicates the presence of an interloper state in the series of states that are analyzed. One can notice that in the present system, where the confined wave

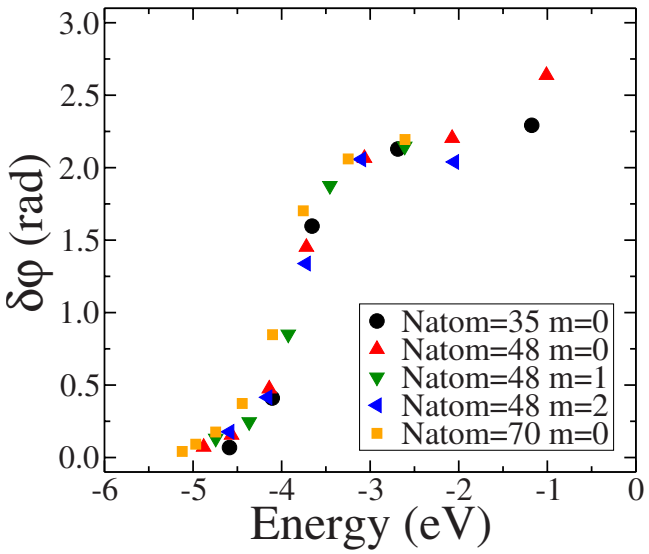

FIG. 7. (Color online) Phase shift of the (m,p) corral states as a function of their energy. Results for a corral with 35 atoms (black circles), 48 atoms ($m=0$: red up triangles; $m=1$: green down triangles; and $m=2$: blue left triangles), and 70 atoms (yellow squares) are shown.

function is a Bessel function, the phase increase because of the extra state should be equal to the difference between two zeros of the J_0 function; however, apart from the first one, the difference between $Z_{m,p}$'s is very close to π and thus this should not influence the discussion. The analysis of the wave functions of the various resonances performed in Sec. III A clearly points at the presence of an extra state in the spectrum appearing in the vicinity of the *sp* state of the Cu wall. However, the phase-shift increase obtained here is smaller than π radians. This is attributed to the simplicity of the model given by Eqs. (10) and (11) which cannot perfectly account for the full range of the detailed energy spectrum.

Thus, one can conclude that a phase analysis of the energy spectrum of the corral states points at the existence of an extra state in the system, which is induced by a perturbing state located in the vicinity of −4 eV. Note that the $\delta\varphi$ increase is spread over several (m,p) states confirming that no single state can be assigned to the *sp* state. The maximum of the slope of $\delta\varphi$ versus the energy occurs at −3.9 eV which is then the estimated position of the perturbing interloper state in the present system (the *sp* band localized on the corral wall). As expected, it is very close to the bottom of the 1D *sp* band in the case of an infinite Cu wire supported on Cu(111) ($E=-4.07$ eV).[37] Small differences can be attributed to changes from a straight atomic line to a bent one. In particular, the corral is a finite closed wire and so should correspond to the case of a quantized 1D *sp* band. An estimate of the latter effect yields an energy upshift around 10 meV. The width of the perturbed region evaluated from the slope of $\delta\varphi$ versus the energy is equal to 0.7 eV. It must be stressed that the width of the perturbed region is the result of both the intrinsic width of the *sp* band (estimated to be in the 0.3 eV range from our study on supported infinite Cu wires[37]) and of the strength of the coupling between the *sp* band and the quantized surface states.

IV. CONCLUSIONS

We have presented the results of a theoretical study of the surface state confinement by circular corrals formed by Cu adatoms on Cu(111). The energies, lifetimes, decay paths, and wave functions of the system resonances have been determined and analyzed for three different corral sizes (35, 48, and 70 atoms). In line with previous works on confined states in various systems, the properties of the confined states with energies close to the bottom of the surface state continuum are similar to those predicted by a simple particle-in-a-box model. However, as a main result of the present work, a strong perturbation in the spectrum of the unoccupied confined surface states is revealed at higher quantization energies: both the energy and the lifetime of the resonances are affected. (i) The level width as a function of the index or equivalently of the energy of the confined states shows a clear Fano profile and (ii) the energy of the confined states cannot be accurately reproduced by a simple particle-in-a-box model, corresponding to the confinement of the 2D-surface state continuum inside the corral.

We have shown that the origin of the observed phenomenon is the strong coupling between the two types of quasi-stationary states appearing in this system: the confined surface states and the *sp*-resonant state localized on the Cu adatoms of the corral wall. Actually, the *sp* state plays the role of an interloper state inside the spectrum of the quantized states arising from the confinement of the 2D-surface state continuum inside the corral. The *sp* state mixes with several confined states leading to a strong perturbation of the spectrum of corral states. Indeed, the *sp* state does not appear as a specific state in the spectrum but rather as a perturbation in a finite energy range of the spectrum of confined states. This is at variance with similar systems on Cu(111) (single Cu adatom and Cu atomic chains) where a specific *sp*-state peak could be observed in the density of electronic states.[31,32,37,38]

Evidence for the existence of the *sp* resonance as well as its properties could be extracted from the analysis of the perturbation it introduces in the spectrum of confined surface states. Both the width of the corral states and the phase analysis of the energy spectrum of the corral states point at the existence of a perturbing state inside the spectrum of confined states around −3.9 eV. This is very close to the energy where the *sp* state can be expected from its energy in finite and infinite Cu chains.[31,32,37] One can stress that both the level width as a function of energy and the phase analysis of the spectrum should be very efficient tools to extract evidence for a resonance localized on a corral wall from experimental results on the confined states.

The corral we considered here [a perfectly circular arrangement of Cu adatoms on Cu(111)] is an idealized structure. However, we expect the phenomena found in the present study to be very general. In particular, we expect electronic states confined in a surface nanostructure made of adatoms to strongly interact with atomic orbitals localized on the edges of the structure. This interaction can lead to various phenomena, depending on the relative value of the energy distance between the confined states and the perturba-

tion range of the atomic orbital. The specificity of the present case is due to the fact that the *sp* resonance can perturb the spectrum over a significant energy range and mixes with several confined states.

ACKNOWLEDGMENT

S.D.-T. gratefully acknowledges the postdoctoral program of the Spanish Ministerio de Educación y Ciencia.

*jean-pierre.gauyacq@u-psud.fr

[1] J. A. Stroscio and D. M. Eigler, Science **254**, 1319 (1991).
[2] M. F. Crommie, C. P. Lutz, and D. M. Eigler, Science **262**, 218 (1993).
[3] E. J. Heller, M. F. Crommie, C. P. Lutz, and D. M. Eigler, Nature (London) **369**, 464 (1994).
[4] J. Kliewer, R. Berndt, and S. Crampin, Phys. Rev. Lett. **85**, 4936 (2000).
[5] H. C. Manoharan, C. P. Lutz, and D. M. Eigler, Nature (London) **403**, 512 (2000).
[6] K.-F. Braun and K.-H. Rieder, Phys. Rev. Lett. **88**, 096801 (2002).
[7] M. C. Desjonquères and D. Spanjaard, *Concepts in Surface Physics* (Springer, Berlin, 1993).
[8] S. Crampin, M. H. Boon, and J. E. Inglesfield, Phys. Rev. Lett. **73**, 1015 (1994).
[9] S. Crampin and O. R. Bryant, Phys. Rev. B **54**, R17367 (1996).
[10] V. S. Stepanyuk, L. Niebergall, W. Hergert, and P. Bruno, Phys. Rev. Lett. **94**, 187201 (2005).
[11] H. K. Harbury and W. Porod, Phys. Rev. B **53**, 15455 (1996).
[12] G. A. Fiete and E. J. Heller, Rev. Mod. Phys. **75**, 933 (2003).
[13] V. S. Stepanyuk, N. N. Negulyaev, L. Niebergall, and P. Bruno, New J. Phys. **9**, 388 (2007).
[14] V. Madhavan, W. Chen, T. Jamneala, M. F. Crommie, and N. S. Wingreen, Science **280**, 567 (1998).
[15] D. Porras, J. Fernandez-Rossier, and C. Tejedor, Phys. Rev. B **63**, 155406 (2001).
[16] J. Li, W.-D. Schneider, R. Berndt, and S. Crampin, Phys. Rev. Lett. **80**, 3332 (1998).
[17] J. Li, W.-D. Schneider, S. Crampin, and R. Berndt, Surf. Sci. **422**, 95 (1999).
[18] S. Pons, P. Mallet, and J.-Y. Veuillen, Phys. Rev. B **64**, 193408 (2001).
[19] L. Diekhöner, M. A. Schneider, A. N. Baranov, V. S. Stepanyuk, P. Bruno, and K. Kern, Phys. Rev. Lett. **90**, 236801 (2003).
[20] J. P. Gauyacq and A. G. Borisov, Surf. Sci. **600**, 825 (2006).
[21] F. Calleja, J. J. Hinarejos, A. L. Vázquez de Parga, and R. Miranda, Eur. Phys. J. B **40**, 415 (2004).
[22] S. Crampin, H. Jensen, J. Kroger, L. Limot, and R. Berndt, Phys. Rev. B **72**, 035443 (2005).
[23] L. Niebergall, G. Rodary, H. F. Ding, D. Sander, V. S. Stepanyuk, P. Bruno, and J. Kirschner, Phys. Rev. B **74**, 195436 (2006).
[24] S. Díaz-Tendero, A. G. Borisov, and J. P. Gauyacq, Phys. Rev. B **76**, 155428 (2007).
[25] E. V. Chulkov, A. G. Borisov, J. P. Gauyacq, D. Sánchez-Portal, V. M. Silkin, V. P. Zhukov, and P. M. Echenique, Chem. Rev. (Washington, D.C.) **106**, 4160 (2006).
[26] P. M. Echenique, R. Berndt, E. V. Chulkov, Th. Fauster, A. Goldmann, and U. Höfer, Surf. Sci. Rep. **52**, 219 (2004).
[27] N. Nilius, T. M. Wallis, and W. Ho, Science **297**, 1853 (2002).
[28] T. M. Wallis, N. Nilius, and W. Ho, Phys. Rev. Lett. **89**, 236802 (2002).
[29] N. Nilius, T. M. Wallis, and W. Ho, Appl. Phys. A: Mater. Sci. Process. **80**, 951 (2005).
[30] N. Nilius, T. M. Wallis, and W. Ho, J. Phys. Chem. B **109**, 20657 (2005).
[31] S. Fölsch, P. Hyldgaard, R. Koch, and K. H. Ploog, Phys. Rev. Lett. **92**, 056803 (2004).
[32] J. Lagoute, X. Liu, and S. Fölsch, Phys. Rev. B **74**, 125410 (2006).
[33] J. Lagoute, X. Liu, and S. Fölsch, Phys. Rev. Lett. **95**, 136801 (2005).
[34] T. Matsui, Chr. Meyer, L. Sacharow, J. Wiebe, and R. Wiesendanger, Phys. Rev. B **75**, 165405 (2007).
[35] V. S. Stepanyuk, A. N. Klavsyuk, L. Niebergall, and P. Bruno, Phys. Rev. B **72**, 153407 (2005).
[36] M. Persson, Phys. Rev. B **70**, 205420 (2004).
[37] S. Díaz-Tendero, F. E. Olsson, A. G. Borisov, and J. P. Gauyacq (unpublished).
[38] F. E. Olsson, M. Persson, A. G. Borisov, J. P. Gauyacq, J. Lagoute, and S. Fölsch, Phys. Rev. Lett. **93**, 206803 (2004).
[39] F. E. Olsson, A. G. Borisov, M. Persson, N. Lorente, A. K. Kazansky, and J. P. Gauyacq, Phys. Rev. B **70**, 205417 (2004).
[40] F. E. Olsson, A. G. Borisov, and J. P. Gauyacq, Surf. Sci. **600**, 2184 (2006).
[41] E. V. Chulkov, V. M. Silkin, and P. M. Echenique, Surf. Sci. **437**, 330 (1999).
[42] G. Kresse and J. Furthmüller, Phys. Rev. B **54**, 11169 (1996).
[43] L. Kleinman and D. M. Bylander, Phys. Rev. Lett. **48**, 1425 (1982).
[44] A. G. Borisov, A. K. Kazansky, and J. P. Gauyacq, Phys. Rev. B **59**, 10935 (1999).
[45] D. Neuhauser and M. Baer, J. Chem. Phys. **91**, 4651 (1989).
[46] M. D. Feit, J. A. Fleck, Jr., and A. Steiger, J. Comput. Phys. **47**, 412 (1982).
[47] R. Kosloff, J. Phys. Chem. **92**, 2087 (1988).
[48] W. H. Press, S. A. Tenkolsky, W. T. Vetterling, and B. P. Flannery, *Numerical Recipes in FORTRAN* (Cambridge University Press, Cambridge, 1992).
[49] A. G. Borisov, J. P. Gauyacq, and S. V. Shabanov, Surf. Sci. **487**, 243 (2001).
[50] P. Nordlander and J. C. Tully, Phys. Rev. B **42**, 5564 (1990).
[51] A. G. Borisov, A. K. Kazansky, and J. P. Gauyacq, Surf. Sci. **430**, 165 (1999).
[52] A. G. Borisov, J. P. Gauyacq, A. K. Kazansky, E. V. Chulkov, V. M. Silkin, and P. M. Echenique, Phys. Rev. Lett. **86**, 488 (2001).
[53] J. P. Gauyacq, A. G. Borisov, and M. Bauer, Prog. Surf. Sci. **82**, 244 (2007).
[54] T. Hakala, M. J. Puska, A. G. Borisov, V. M. Silkin, N. Zabala, and E. V. Chulkov, Phys. Rev. B **75**, 165419 (2007).
[55] U. Fano, Phys. Rev. **124**, 1866 (1961).

[56] A. G. Borisov, J. P. Gauyacq, E. V. Chulkov, V. M. Silkin, and P. M. Echenique, Phys. Rev. B **65**, 235434 (2002).
[57] F. Theilmann, R. Matzdorf, G. Meister, and A. Goldmann, Phys. Rev. B **56**, 3632 (1997).
[58] J. Kliewer, R. Berndt, E. V. Chulkov, V. M. Silkin, P. M. Echenique, and S. Crampin, Science **288**, 1399 (2000).
[59] F. Reinert, G. Nicolay, S. Schmidt, D. Ehm, and S. Hüfner, Phys. Rev. B **63**, 115415 (2001).
[60] L. Bürgi, O. Jeandupeux, H. Brune, and K. Kern, Phys. Rev. Lett. **82**, 4516 (1999).
[61] H. Friedrich and D. Wintgen, Phys. Rev. A **31**, 1920 (1985).
[62] U. Fano, Phys. Rev. A **37**, 4037 (1988).